



Contents lists available at ScienceDirect

Journal of King Saud University – Science

journal homepage: www.sciencedirect.com

Original article

Copper oxide nanoparticles synthesized from *Trichosanthes kirilowii* ameliorates the DSS-induced acute colitis in mice through the suppression of inflammatory responses

Xuefeng Jiang^a, Yu Sun^b, Tahani Awad Alahmadi^c, Velu Manikandan^d, Thamaraiselvan Rengarajan^e, Yuyang Zhao^{a,*}^a Department of Gastroenterology, China-Japan Union Hospital of Jilin University, Changchun, Jilin 130033, China^b Department of Interventional Radiology, China-Japan Union Hospital of Jilin University, Changchun 130033, China^c Department of Pediatrics, College of Medicine and King Khalid University Hospital, King Saud University, Medical City, PO Box-2925, Riyadh 11461, Saudi Arabia^d Division of Biotechnology, College of Environmental and Bioresource Sciences, Jeonbuk National University, Iksan 54596, South Korea^e SCIGEN Research and Innovation Pvt. Ltd., Periyar Technology Business Incubator, Thanjavur, Tamil Nadu, India

ARTICLE INFO

Article history:

Received 11 June 2021

Revised 27 October 2021

Accepted 30 December 2021

Available online 5 January 2022

Keywords:

Copper nanoparticles

Ulcerative colitis

Inflammation

COX-2

iNOS

Trichosanthes kirilowii

ABSTRACT

Introduction: Ulcerative colitis (UC) is chronic inflammatory ailment that distinguished by diarrhea, stomach pain, reduced body weight, and hematochezia. UC affects nearly 400 per 100,000 peoples worldwide. In this exploration, we intended to fabricate the copper oxide nanoparticles from the *T. kirilowii* (TK-CuNPs) and inspect their curative potential against the Dextran sulfate disodium salt (DSS)-provoked colitis in animals.

Methods: Formulated TK-CuNPs were characterized by UV–vis spectroscopy, FT-IR, SEM, TEM, and DLS techniques. UC was provoked in mice through administering of 2% DSS for 7-days and treated with the 10 mg/kg bodyweight of TK-CuNPs via intragastric intubation. Myeloperoxidase activity, colon weight, and length, and spleen weight were determined by standard methods. Pro-inflammatory mediators, i.e. IL-6, IL-1 β , and TNF- α were inspected by the assay kits. The expression of COX-2 and iNOS were analyzed by immunohistochemistry. Histopathological changes in colon tissues were investigated microscopically by H&E staining. The cytotoxicity and *in vitro* anti-inflammatory activities of TK-CuNPs were analyzed in RAW-264.7 cells.

Results: The outcomes of various characterization studies demonstrated the formation of TK-CuNPs. The TK-CuNPs supplementation to the DSS induced colitis mice demonstrated the appreciable bodyweight gain and reduced the DAI scores. TK-CuNPs improved the colon length and spleen weight and suppressed the MPO activity. The status of pro-inflammatory mediators IL-6, IL-1 β , and TNF- α was appreciably suppressed by the TK-CuNPs treatment. The expressions of COX-2 and iNOS was also diminished by the TK-CuNPs. TK-CuNPs did not possessed toxicity to the RAW-264.7 cells and suppressed the inflammatory markers level in the RAW-264.7 cells.

Discussion and Conclusion: The current findings revealed that fabricated TK-CuNPs can be a hopeful therapeutic agent to treat acute colitis.

© 2021 Published by Elsevier B.V. on behalf of King Saud University. This is an open access article under the CC BY-NC-ND license (<http://creativecommons.org/licenses/by-nc-nd/4.0/>).

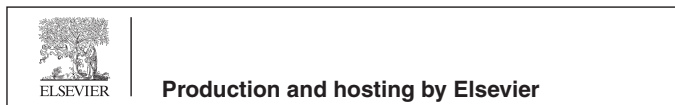
1. Introduction

Inflammatory bowel disease (IBD) is a persistent inflammatory ailment in the gastrointestinal tracts, which is caused by the augmented pro-inflammatory mediators and epithelial barrier dysfunctions. Numerous ailments like IBD are associated with intestinal functional disorders (Hagenlocher et al., 2016). IBD usually incorporates Crohn's disease (CD) and ulcerative colitis (UC), which is a chronic inflammatory ailment that affects the gastrointestinal tract and accounts for nearly 400 per 100,000 incidences

* Corresponding author.

E-mail address: zhaoyuyang@jlu.edu.cn (Y. Zhao).

Peer review under responsibility of King Saud University.

<https://doi.org/10.1016/j.jksus.2021.101817>

1018-3647/© 2021 Published by Elsevier B.V. on behalf of King Saud University.

This is an open access article under the CC BY-NC-ND license (<http://creativecommons.org/licenses/by-nc-nd/4.0/>).

worldwide. There is a rapid upsurge in the occurrence of IBD around the world which indicates the emergence of IBD as a universal ailment. The pathogenesis of IBD involves dysregulation and stimulation of mucosal immune reactions that eventually disturb the barrier integrity, which leads to the augmented permeability of colon epithelial, and up-regulated pro-inflammatory cytokine expressions and oxidative stress (Michielan and D'Inca, 2015).

Nuclear factor- κ B (NF- κ B) is an imperative mediator of the inflammatory reactions and is accountable for the excessive accretion of pro-inflammatory arbitrators that are crucial for the pathogenesis of chronic inflammatory ailments like UC. Thus, the NF- κ B translocation into the nucleus triggers the inflammatory reactions and further triggers the transcription of inflammatory arbitrators, i.e. TNF- α , IL-1 β , COX-2, iNOS, and IL-6 (Chae et al., 2017). It is well known that the enhancement of some enzymes like iNOS, COX-2, and excessive accretion of pro-inflammatory regulators plays a vital functions in the development of UC (Katsanos and Papadakis, 2017). During the progression of UC, the proinflammatory arbitrators like TNF- α and IL-6 are augmented in the colonic mucosa, which eventually leads to severe inflammatory conditions (Naraginti et al., 2016). Inflammatory responses enhance the oxidative stress via triggering reactive oxygen species (ROS)-accreting systems, like iNOS, and myeloperoxidase (MPO). These are intimately implicated in inflammatory mediators and penetration of leucocytes through triggering the NF- κ B cascade in IBD (Zhu and Li, 2012).

Recently, nanotechnology has emerged in the medical field with extensive application to treat the ailments. Salutary nanoparticles (NPs) have provided remarkable advantages in IBD treatment (Uranga et al., 2016). The copper nanoparticles are studied extensively in the medical field due to their versatility. It was already highlighted that the copper NPs possessed the exclusive antimicrobial, antioxidant, and anticancer activities, which makes them a hopeful tool for biomedical utilizations (Li et al., 2017; Maqbool et al., 2017). The absence of targeted drug delivery and insufficient drug availability at the selected sites influences in patients to treat colon cancer. Drug nanoformulations overwhelmed the general obstacles inflicted by the colon like thicker mucus layer and disturbed epithelium (Mohammed et al., 2018). Numerous nano sized drug delivery evidenced more potential in IBD animal models (Beloqui et al., 2016).

Trichosanthes kirilowii is extensively utilized in East Asian nations as a cough-suppressive and anti-diabetic agent. *T. kirilowii* has revealed the renoprotective action against cisplatin-induced nephrotoxicity (Seo et al., 2015). A study by Liu et al. (2012) showed that trichosanthin from *T. kirilowii* prevented the multiplication of nasopharyngeal cancer cells. *T. kirilowii* was found to be effective against breast cancer (Kim et al., 2013). It was previously reported that the gold nanoparticles synthesized *T. kirilowii* also exhibits anticancer activity against the colon cancer cell (Han et al., 2019). Hence, in this exploration, we planned to synthesize the copper oxide nanoparticles from the *T. kirilowii* leaf extract and inspect its curative potential against the dextran sulfate sodium (DSS)-challenged UC in animals via suppression of inflammatory responses.

2. Materials and methods

2.1. Chemicals

Copper acetate, DSS (molecular weight: 726.6 g/mol), and other chemicals were procured from Sigma-Aldrich, USA. All the ELISA kits were obtained from Invitrogen, USA. All other chemicals and reagents were obtained from Himedia, USA.

2.2. Preparation of plant extract

Around 5 g of *T. kirilowii* leaf was weighed and suspended in the 100 ml of pure water and heat-macerated for 30 mins at 60 °C. After that, suspension were filtered using the Whatman filter paper, and finally, extract was consumed to synthesize the copper NPs.

2.3. Synthesis of copper nanoparticles (CuNPs)

The synthesis of CuNPs were done by using the previous procedure described by Harne et al. (2012). Briefly, 10 ml of extract were mixed to the 190 ml of 5 mM copper acetate solution and heated for 80 °C with continual stirring for 30 min. The bio reduction of copper acetate in the extract containing reaction medium resulted in the generation of CuNPs. After the incubation, the CuNPs in the reaction mixture was pelleted via centrifugation at 6000 rpm for 7 min. The synthesized CuNPs were utilized for several characterization studies.

2.4. Characterization of synthesized CuNP's

2.4.1. UV-vis spectroscopic analysis

For the confirmation of the bioreduction of CuNPs in the sample, the UV-vis spectroscopic study was executed (Shimadzu-1700, Japan). The bioreduction of CuNPs was evidenced using the UV spectrometric study, and the absorbance was taken at 200–600 nm.

2.4.2. Fourier Transform-Infrared (FT-IR) analysis

FT-IR study was performed to inspect the existence of functional groups on the surface of the synthesized CuNPs. Briefly, the dried and powdered form of synthesized CuNPs was analyzed using the FT-IR analysis (Shimadzu-8400S, Japan). The spectrum of FT-IR of synthesized CuNPs was obtained by the potassium bromide (KBr) disc technique. The spectrum of FT-IR was inspected over the range of (4000–400 cm⁻¹) with the resolution at 4 cm⁻¹ for 50 scans.

2.4.3. Scanning electron microscopic (SEM) analysis

The size and morphology of the fabricated CuNPs was studied through the SEM under the average atmospheric conditions. The synthesized CuNPs were investigated through the SEM machine (ZEISS-Supra-40, Germany) at the 5 kV. The CuNPs were placed on the clean glass slide and spread uniformly and vacuum dried. Finally, the sample was inspected through SEM under a high vacuum and at various magnifications.

2.4.4. Transmission electron microscopic (TEM) analysis

The fabricated CuNPs were investigated by using the TEM analysis to detect the size and distribution. TK-CuONPs were located on the carbon painted copper grid and dehydrated for 30 min. after that grid was loaded with the TK-CuNPs and then located on the sample holder. Lastly, the microscopic images of TK-CuNPs were taken via TEM instrument (JOEL JSM 100CX TEM, Japan) operating by accelerating voltage 200 kV.

2.4.5. Dynamic light scattering (DLS) assay

The fabricated TK-CuNPs were examined by the analysis to measure the average size and distribution patterns. The TK-CuNPs were analyzed through the DLS equipment Zeta sizer (Malvern, USA).

2.5. In-vitro anti-inflammatory effects of formulated TK-CuNPs

2.5.1. Collection of cell line

Murine macrophage (RAW 264.7) cells were attained from ATCC, USA and sustained in DMEM medium enriched with 10% of FBS and 1% of antimycotic mixture in a moistened chamber with CO₂ (5%) at 37 °C. The cells were replenished with new medium for every 2–3 days.

2.5.2. Cell viability assay

The toxic level of formulated TK-CuNPs on the RAW-264.7 cells were assessed through the MTT assay. RAW-264.7 cells were loaded in 96-well plate at 1×10^5 (Katsanos and Papadakis, 2017) cells/well density and maintained for 24 h then treated with LPS (100 ng/ml) along with different doses of (2.5, 5.0, 7.5, 10, and 12.5 μ M) of fabricated TK-CuNPs and incubated for another 24 h. After that, 10 μ l of MTT reagent was mixed to all the wells and nurtured for 4 h at 37 °C. Then medium was eliminated and 100 μ l of DMSO was mixed to liquefy the formazan crystals. Finally, the absorbance was readed at 570 nm in microplate reader.

2.5.3. Determination of pro-inflammatory cytokines and ROS levels in RAW-264.7 cells

RAW-264.7 cells were plated on 24 well-plate at 5×10^5 (Katsanos and Papadakis, 2017) cells/well population and supplemented with fabricated TK-CuNPs at diverse doses (2.5, 5.0, and 7.5 μ M) and sustained for 1 h at 37 °C. Then RAW-264.7 cells were challenged with 100 ng/ml of LPS for 18 h and then medium was removed and the cells suspension was gathered for the measurement of pro-inflammatory mediators status like TNF- α and IL-6 by using specific kits (Santacruz, USA). The nitric oxide (NO) status was examined via the Griess reagent (Sigma-Aldrich, USA) with sodium nitrite as standard. For the measurement of intracellular ROS level, the cells were cleansed with PBS and stained by 10 mM/L of DCF-DA for 30 min in dark condition. The level of ROS accumulation was measured by measuring at 485 nm excitation and 535 nm emission (Lautraite et al., 2003).

2.6. Experimental animals

Male Balb/c mice (7 weeks aged) weighing 21 ± 3 g were attained from Institutional animal house. All animals were maintained in organized laboratory conditions, i.e. temperature 26 ± 1 °C, 60 – 70% humidity, dark and light series were 12 h. All animals were administered with commercial pellet food with water ad libitum. The treatment procedures were completed as per the standard guidelines by the National Institutes of Health, United States.

2.7. Experimental design

Animals were separated into four groups (n = 6/group). Group-I (Control) were given drinking water without DSS for 7 days, Group-II (DSS control group) were administered 2 % (w/v) of DSS for 7 days. Group-III animals received oral administration of 10 mg/kg of TK-CuNPs along with DSS for 7 days. Group-IV animals were orally administered with standard drug Sulfasalazine (50 mg/kg) through oral gavage along with DSS. After the end of experiments, animals were anesthetized and fortified via cervical dislocation, and then samples were gathered for additional assays.

2.8. Assessment of disease activity index (DAI) scores

DAI scores of the investigational mice were inspected via daily monitoring for UC signs, i.e. bodyweight, stool consistency, and rectal bleeding. DAI was allocated as per the scoring system, as suggested by Cooper et al. (1993). (a) weight loss: (0 for none, 1

for 1–5%, 2 for 5–10%, 3 for 10–15%, and 4 for more than 15%; (b) consistency of stool: 0 for normal, 2 for loose stools, 4 for watery diarrhea; and (c) bleeding: 0 for no bleeding, 2 for slight bleeding, and 4 for gross bleeding. The DAI was determined as a sum of these scores.

2.9. Determination of myeloperoxidase (MPO) enzyme activity

The enzymatic action of MPO in the colon tissues of control and TK-CuNPs treated animals were estimated using the protocol of Mullane et al. (1985). The gathered colon tissues were homogenized with the 0.1 M phosphate buffer (pH-6.5) to attain 5% of homogenate. Then the suspension was centrifuged at 12,000 rpm for 10 min. Around 0.12 ml of supernatant was mixed with 2.9 ml of the reaction solution, consisting of 0.005 % of hydrogen peroxide and 0.16 mg/ml of o-dianisidine hydrochloride. Then the reaction solution was incubated for 5 min; and the absorbance was taken at 460 nm.

2.10. Assessment of pro-inflammatory mediators in the colon tissue

The IL-6, IL-1 β , and TNF- α levels in the control and TK-CuNPs administered colitis animals were investigated by using the relevant assay kits as per the manufacturer's instructions (MyBioSource, USA).

2.11. Immunohistochemical analysis of iNOS and COX-2 expression in the colon tissue

Paraffin-embedded colon tissues were incised at 5 μ m size and the tissues were processed with 0.5% of TritonX-100 at 37 °C for 30 min. Then tissues were blocked with BSA (2%) for 1 h at 37 °C and incubated with primary antibodies (iNOS and COX-2) (1:100) overnight at 37 °C. Subsequent to cleansing twice with PBS, tissues were again incubated with HRP-conjugated goat anti-rabbit antibodies at 37 °C for 30 min, followed by counterstaining with hematoxylin. Then tissues were observed beneath microscope and images were taken.

2.12. Histopathological analysis

The excised colon tissues were cleansed with 10% of formalin. Then the tissues were entrenched in the paraffin. The paraffinized tissues were incised into 5 μ m size and stained with H&E. Finally, tissues were investigated by using an microscope at 40 \times magnification, and histological changes in the colon tissues of investigational animals were detected.

2.13. Data analysis

Values were assessed statistically using Graph pad prism software (version 5.0). Outcomes were represented as mean \pm SD of triplicates. One-way ANOVA and DMRT analysis was executed to test the variations between groups. The significance was fixed at $p < 0.05$.

3. Results

3.1. UV-vis spectral analysis of formulated TK-CuNPs

The bio reduction of Cu⁺ ions may result in the generation of CuNPs in the solution, and this NPs display the dark color. The synthesized TK-CuNPs were studied through a UV-vis spectrophotometer for confirming the generation of CuNPs (Fig. 1A). The bio reduction of CuNPs in the reaction solution was examined via the UV-vis spectrophotometer by taking the absorbance at various

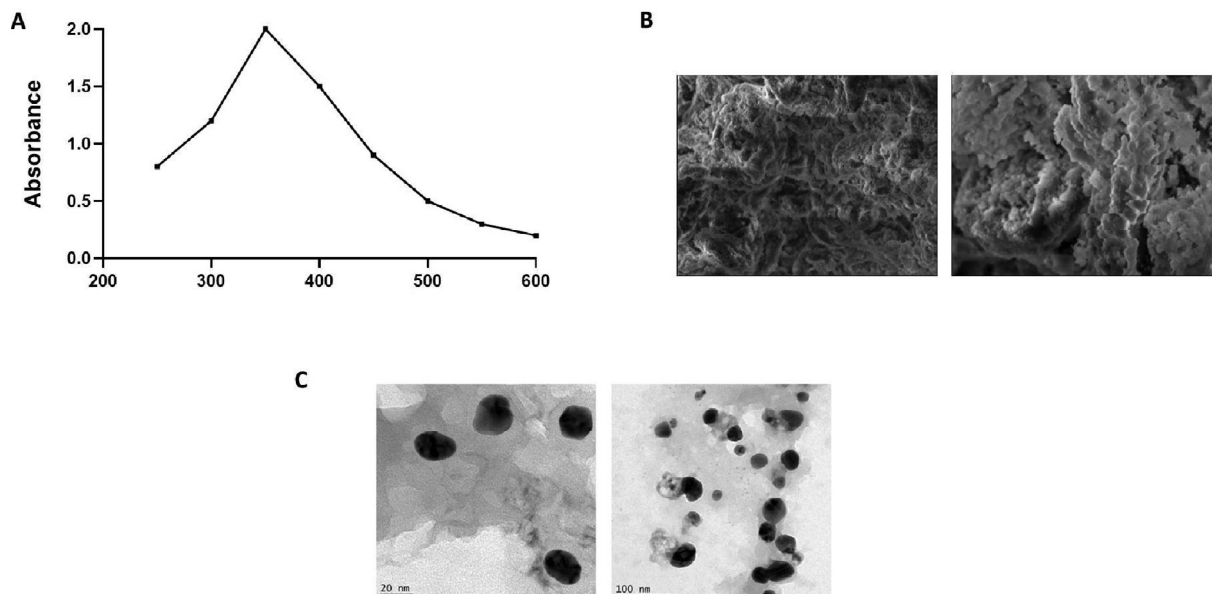


Fig. 1. Characterization analysis of TK-CuNPs. UV-Vis absorption spectrum of formulated TK-CuNPs. The peak values for UV-Vis plotted between TK-CuNPs/absorbance ratios. The highest peak was noted at 340 nm. A. The SEM inspection of synthesized TK-CuNPs displayed the morphology of synthesized TK-CuNPs having the spherical and some particles having irregular structures. B. The TEM investigation of fabricated TK-CuNPs demonstrated the uniformed sized and distribution of TK-CuNPs exhibiting the spherical and somewhat irregular shapes.

wavelengths ranging from 200 to 600 nm. Fig. 1 shows that the highest peak was at 340 nm that eventually proved the generation of CuNPs.

3.1.1. SEM analysis of synthesized TK-CuNPs

The magnitude and the morphology of the synthesized TK-CuNPs were examined through the SEM and results illustrated in Fig. 1B. The microscopic photographs of formulated TK-CuNPs displayed that the synthesized TK-CuNPs were well dispersed in nature and primarily had the spherical morphology, while few NP's displayed uneven shapes as depicted in Fig. 3.

3.1.2. TEM analysis of synthesized TK-CuNPs

The size and distribution of the fabricated TK-CuNPs were examined by using the TEM examination and images were illustrated in Fig. 1C. TEM images of formulated TK-CuNPs was evidenced the existence of TK-CuNPs in a dispersed form with rounded shapes. TEM analysis also proved that the fabricated TK-CuNPs has the circular shapes.

3.2. FT-IR analysis of synthesized TK-CuNPs

The bending and stretching frequencies of molecular functional groups, which are exclusively bound at the exterior of fabricated TK-CuNPs were examined using the FT-IR spectrophotometry. Fig. 2A represents the FT-IR spectrum of formulated TK-CuNPs, and it reveals the numerous absorption peaks at different frequencies. The peak at 3701.89 cm^{-1} denotes a strong band that is attributable to the O-H (hydroxyl) stretching in the surface of TK-CuNPs. The peak at the 2995.79 cm^{-1} indicates the existence of Cu-H stretching and the 1846.84 cm^{-1} , 1489.60 cm^{-1} , and 1302.58 cm^{-1} peak denotes the bending vibrations of C-H and C-O bonds. The peaks at the 706.20 cm^{-1} and 583.52 cm^{-1} denote the Cu-O bonds. On the whole, these peaks depict the generation of CuNPs in the reaction solution (Fig. 2).

3.2.1. DLS analysis of synthesized TK-CuNPs

The DLS examination was executed to detect the size and distribution range of formulated TK-CuNPs (Fig. 2B). The findings of DLS

analysis demonstrated the single peak with a size of ranged from 959.1 nm and a narrow distribution.

3.3. Effect of TK-CuNPs on the cell viability of RAW 264.7 cells

The cell viability of TK-CuNPs supplemented RAW-264.7 cells were studied through the MTT assay. The control cells did not showed any cell death. Interestingly, the TK-CuNPs supplemented cells also possessed no cell death up to the $7.5\text{ }\mu\text{M}$ concentration (Fig. 3). However, the $10\text{ }\mu\text{M}$ of TK-CuNPs exhibited very mild cytotoxicity to RAW 264.7 cells. There are no variations on the cell viability between the control and TK-CuNPs treated cells up to the $7.5\text{ }\mu\text{M}$ concentration and demonstrated the similar outcomes, which proves that these concentration of TK-CuNPs are not cytotoxic to RAW 264.7 cells (Fig. 6). Hence the 2.5 , 5.0 , & $7.5\text{ }\mu\text{M}$ of TK-CuNPs were opted for further studies.

3.4. Effect of TK-CuNPs on the status of pro-inflammatory cytokines and ROS in LPS-challenged RAW-264.7 cells

The status of pro IL-6 and TNF- α and ROS was drastically augmented in the LPS-triggered RAW-264.7 cells, which is in contrast to control cells. Surprisingly, the treatment with the formulated TK-CuNPs to the LPS-challenged RAW 264.7 cells were displayed the notable diminution in the IL-6, TNF- α , and ROS statuses, when related to the LPS alone administered cells. TK-CuNPs appreciably decreased the IL-6, TNF- α , and ROS statuses in the LPS-challenged RAW-264.7 cells (Fig. 4). These outcomes proved that the TK-CuNPs possessed the potent anti-inflammatory activity.

3.5. Effect of TK-CuNPs on the bodyweight and DAI in the colitis mice

The reduced body weight and augmented DAI scores were noticed in the DSS-activated colitis mice than the control. As depicted in Fig. 5, the TK-CuNPs treatment appreciably improved the bodyweight of the colitis mice. The DAI scores were also reduced in DSS induced TK-CuNPs supplemented group. The supplementation of TK-CuNPs has remarkably regained the bodyweight and diminished the DAI scores in the DSS-induced colitis

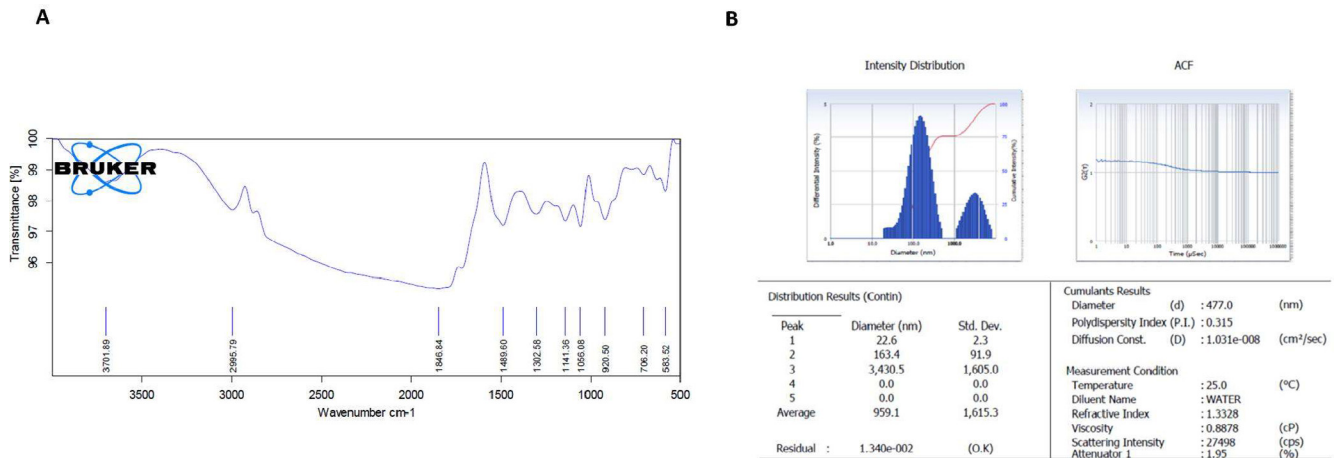


Fig. 2. Fourier-transform infrared spectroscopy and Dynamic light scattering (DLS) analysis of TK-CuNPs. A. The FT-IR spectral study of synthesized TK-CuNPs was evidenced by the existence of O–H, Cu–H, C–H, C–O, and Cu–O stretching that was confirmed by different peaks. B. The average size of the formulated TK-CuNPs was analyzed through DLS and it demonstrated that the Z average diameter was 959.1 nm.

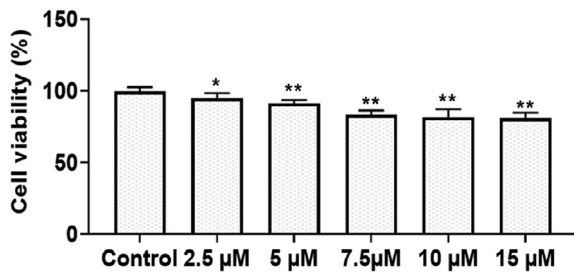


Fig. 3. Effect of TK-CuNPs on the cell viability of RAW 264.7 cells. Values were illustrated as mean ± SD of triplicates. Significance was determined by one-way ANOVA and DMRT assay; *&**p < 0.05 when evaluated with control cells.

mice (Fig. 8). Sulfasalazine treatment also recovered the body-weight and reversed the DAI scores in colitis mice. Similar outcomes were observed between the TK-CuNPs, sulfasalazine, and control animals.

3.6. Effect of TK-CuNPs on the colon weight and length in the colitis animals

The DSS-induced mice revealed a marked reduction in both weight and length of the colon, compared to control mice. Administration of TK-CuNPs (10 mg/kg) to the colitis mice exhibited normal colon length and weight compared to the DSS-triggered mice (Fig. 6). Supportively, the Sulfasalazine (50 mg/kg) administration also improved the weight and length of the colon.

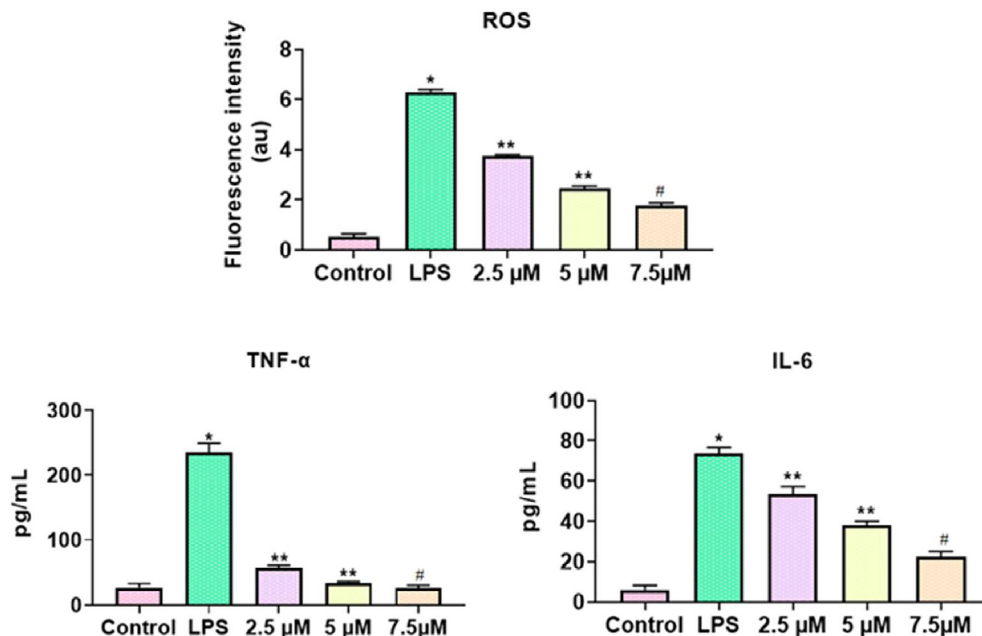


Fig. 4. Effect of TK-CuNPs on the status of pro-inflammatory cytokines and ROS in LPS-challenged RAW-264.7 cells. Values were illustrated as mean ± SD of triplicates. Significance was determined by one-way ANOVA and DMRT assay; *&**p < 0.05 when evaluated with control, **p < 0.05 when evaluated with the DSS-challenged group, #p < 0.001 when evaluated with TK-CuNPs-treated group. Note: Group I: Normal control animals, Group II: DSS-induced colitis animals, Group III: DSS-induced animals treated with 10 mg/kg of TK-CuNPs, Group IV: DSS-provoked and Sulfasalazine (50 mg/kg) treated animals.

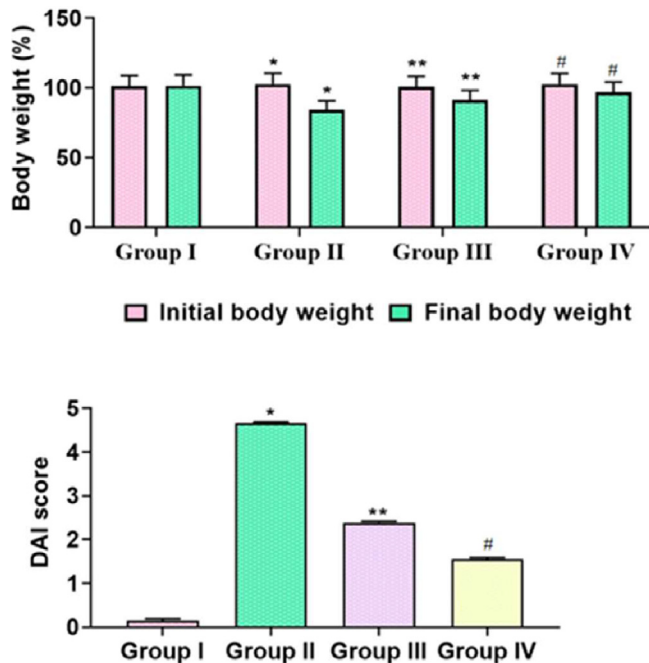


Fig. 5. Effect of TK-CuNPs on the bodyweight and disease activity index (DAI) in the DSS-induced colitis mice. Values were illustrated as mean ± SD of triplicates. Significance was determined by one-way ANOVA and DMRT assay; * & ** p < 0.05 when evaluated with control, ** p < 0.05 when evaluated with the DSS-challenged group, # p < 0.001 when evaluated with TK-CuNPs-treated group. Note: Group I: Normal control animals, Group II: DSS-induced colitis animals, Group III: DSS-induced animals treated with 10 mg/kg of TK-CuNPs, Group IV: DSS-provoked and Sulfasalazine (50 mg/kg) treated animals.

3.7. Effect of TK-CuNPs on the spleen weight and myeloperoxidase (MPO) activity in the colitis mice

The augmented activity of MPO and increased spleen weight was noted in the DSS-triggered mice when related with control (Fig. 7). The treatment with formulated TK-CuNPs (10 mg/kg) remarkably reduced the enzymatic activity of MPO and spleen weight in the DSS-challenged colitis mice related to that of DSS only challenged

mice. TK-CuNPs markedly repressed MPO activity and suppressed the spleen weight, which is similar to the control group (Fig. 10). Sulfasalazine administered mice also displayed a reduced activity of MPO and reduced spleen weight in the colitis mice.

3.8. Effect of TK-CuNPs on the status of pro-inflammatory markers in the colitis mice

As depicted in Fig. 11, an escalated amount of pro-inflammatory arbitrators, i.e. IL-6, IL-1β, and TNF-α were observed in the serum of DSS-triggered mice than control mice (Fig. 11). TK-CuNPs administered colitis mice unveiled marked reduction in the IL-6, IL-1β, and TNF-α as compared to DSS only challenged mice (Fig. 8). This result showed the anti-inflammatory efficacy of the formulated TK-CuNPs. Sulfasalazine administered colitis mice disclosed a drastic suppression of IL-6, IL-1β, and TNF-α in DSS-incited colitis mice.

3.9. Effect of TK-CuNPs on the colon histology of DSS-challenged mice

DSS-provoked mice had damaged epithelial and mucosal lining while the control mice revealed the typical cellular arrangements. Severe inflammation in the mucosal area, loss in shape of crypts, fibrosis, and infiltration of leucocytes were noticed in the colon tissues. Interestingly, the normal tissue architectures, epithelial linings, and cellular arrangements were observed in the TK-CuNPs supplemented colitis mice (Fig. 9). The TK-CuNPs supplementation prevented the permeation of inflammatory cells and mucosal damage. The average levels of intestinal tissue integrity and epithelial linings were noted in the TK-CuNPs supplemented colitis mice. Sulfasalazine administered colitis mice illustrated the protective effects against the DSS-induced ulceration. A similar kind of outcome was observed between control, TK-CuNPs, and Sulfasalazine administered colitis mice.

3.10. Effect of TK-CuNPs on the expression of COX-2 in the colon tissues of colitis mice

The immunohistochemical study exhibited the up-regulated expression of COX-2 in the DSS-incited mice related to the control.

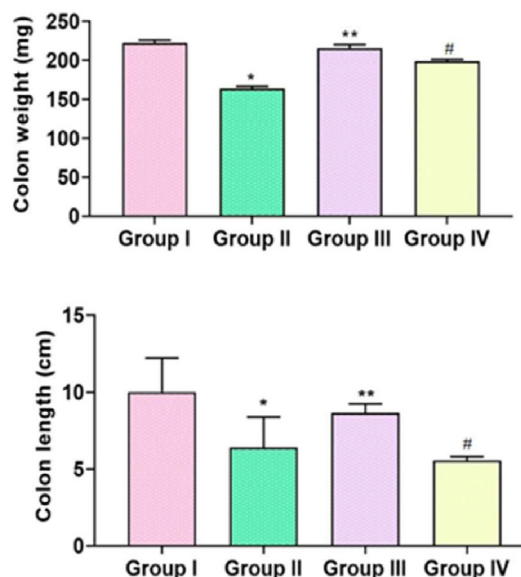
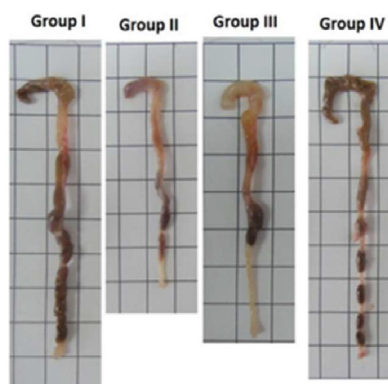


Fig. 6. Effect of TK-CuNPs on the colon weight and length in the DSS-challenged colitis animals. Values were illustrated as mean ± SD of triplicates. Significance was determined by one-way ANOVA and DMRT assay; * & ** p < 0.05 when evaluated with control, ** p < 0.05 when evaluated with DSS-challenged group, # p < 0.001 when evaluated with TK-CuNPs-treated group. Note: Group I: Normal control animals, Group II: DSS-induced colitis animals, Group III: DSS-induced animals treated with 10 mg/kg of TK-CuNPs, Group IV: DSS-provoked and Sulfasalazine (50 mg/kg) treated animals.

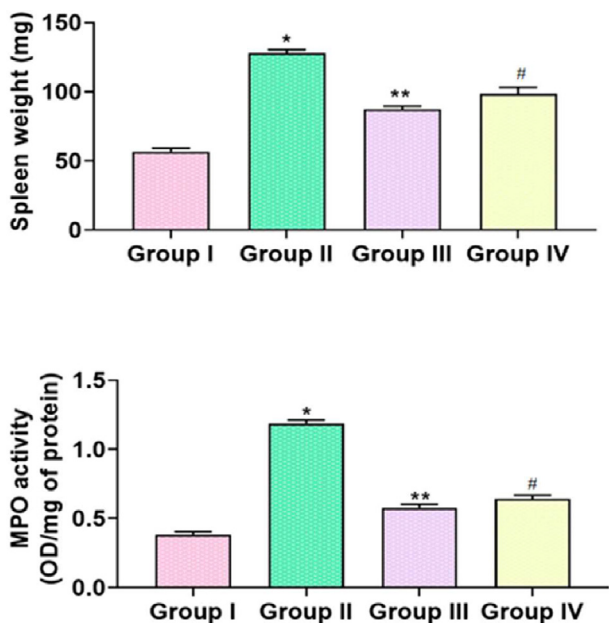


Fig. 7. Effect of TK-CuNPs on the spleen weight and MPO activity in the DSS-challenged colitis mice. Values were illustrated as mean ± SD of triplicates. Significance was determined by one-way ANOVA and DMRT assay; * & ** p < 0.05 when evaluated with control, ** p < 0.05 when evaluated with the DSS-challenged group, # p < 0.001 when evaluated with TK-CuNPs-treated group. Note: Group I: Normal control animals, Group II: DSS-induced colitis animals, Group III: DSS-induced animals treated with 10 mg/kg of TK-CuNPs, Group IV: DSS-provoked and Sulfasalazine (50 mg/kg) treated animals.

DSS-challenged colitis in mice displayed an augmented COX-2 expression. Interestingly, the TK-CuNPs administered colitis mice displayed over-expression of COX-2. The sulfasalazine treated colitis mice also showed reduced expression of COX-2 (Fig. 10). A comparable outcome was noted in between control, TK-CuNPs, and Sulfasalazine administered colitis animals.

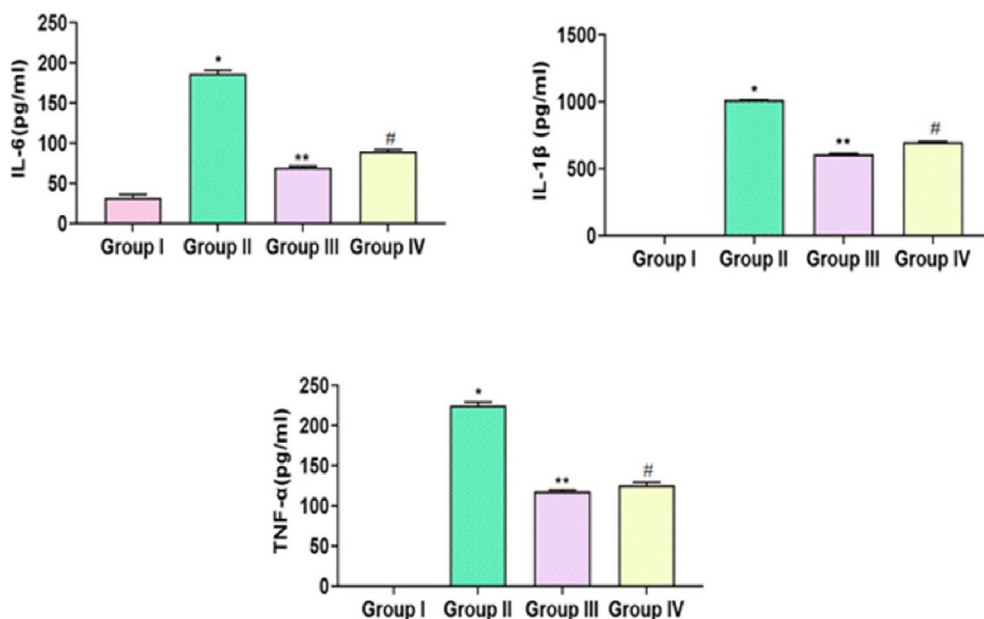


Fig. 8. Effect of TK-CuNPs on the level of the pro-inflammatory marker in the DSS-induced colitis mice. Values were illustrated as mean ± SD of triplicates. Significance was determined by one-way ANOVA and DMRT assay; * & ** p < 0.05 when evaluated with control, ** p < 0.05 when evaluated with the DSS-challenged group, # p < 0.001 when evaluated with TK-CuNPs-treated group. Note: Group I: Normal control animals, Group II: DSS-induced colitis animals, Group III: DSS-induced animals treated with 10 mg/kg of TK-CuNPs, Group IV: DSS-provoked and Sulfasalazine (50 mg/kg) treated animals.

3.10.1. Effect of TK-CuNPs on the expression of iNOS in the colon tissues of colitis mice

Augmented expression of iNOS was noted in the colon tissues of DSS-challenged mice when related to control. DSS-challenged colitis mice illustrated an up-regulated expression of iNOS. The treatment with the TK-CuNPs diminished the expression of iNOS in the DSS-challenged colitis mice (Fig. 10). Sulfasalazine administration also triggered over-expression of iNOS.

4. Discussion

IBD is a chronic and deteriorating inflammatory condition that affects more than millions of people globally (Cosnes et al., 2011). It was reported that the DSS-induced experimental animals demonstrated multiple organ failure and excessive generation of ROS (Balmus et al., 2016). Nanoparticles and nanomedicine are considered as a hopeful remedial tool in gastroenterology. The numerous kinds of nanoparticles have the potential usages in the gastroenterology as they conquer the synthetic drugs in various ailments (Riasat et al., 2016). DSS administration results in diarrhea, bloody stool, and severe ulceration, diminution of body-weight, and shortage of colon length. DSS causes infiltration of intestinal cells to the lumen leading to bloody stool and diarrhea. The reduced colon length and weight are the pathological evidence of UC, which is indicative of the side-effects of IBD (Mizoguchi et al., 2020). In this study, we also noticed the diminished body-weight and DAI scores, decreased colon length and weight, increased spleen weight in the DSS-challenged mice. However, the treatment with the TK-CuNPs in the colitis mice has exhibited improved bodyweight and reduced DAI scores, improved colon length and weight, and decreased spleen weight. These outcomes prove the attenuating potential of fabricated TK-CuNPs against DSS induced pathological alterations in mice. This outcome was coincides with the previous finding (Harne et al., 2012).

The antioxidant enzymes can guard the cells against the injuries of oxidative stress and are regarded as prime scavengers of ROS (Tian et al., 2017). Additionally, MPO is an enzyme, and its level is comparative to the number of neutrophils (Lazarevic-Pasti

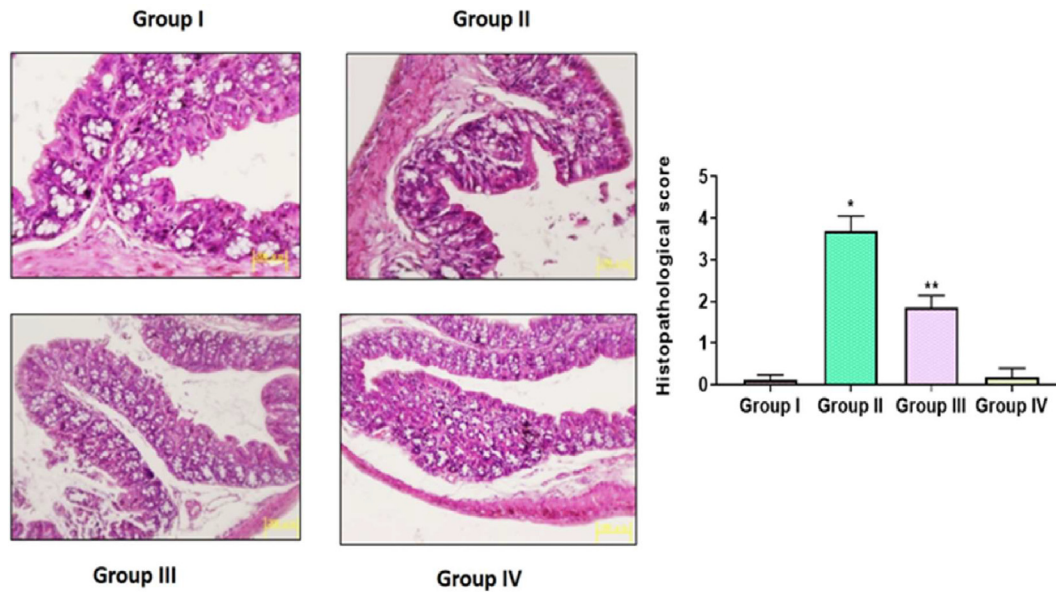


Fig. 9. Effect of synthesized TK-CuNPs on the colon histology in the DSS-stimulated colitis mice. Untreated control animals illustrated normal tissue architecture (Group I). DSS-challenged animals exhibited leucocytes infiltration, inflammation, and severe ulceration in the colon tissues (Group II). The synthesized TK-CuNPs administered mice revealed the nearly normal tissue structures with mild ulceration (Group III). Sulfasalazine administered mice also demonstrated the nearly normal tissue structures (Group IV).

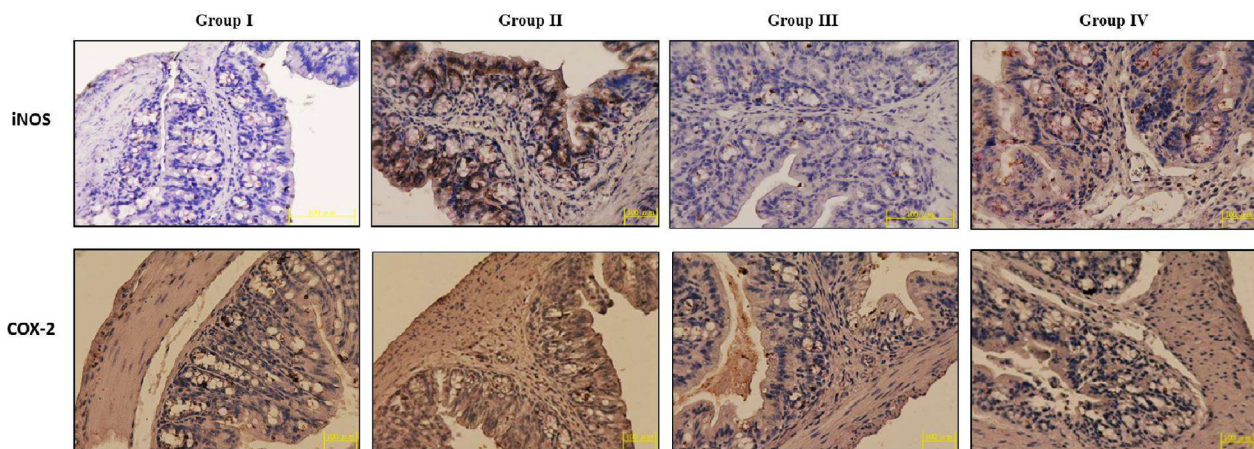


Fig. 10. Effect of TK-CuNPs on the expression of COX-2 and iNOS in the colon tissues of DSS-provoked colitis mice. Untreated control mice showed the mild COX-2 and iNOS expression (Group I). DSS-provoked mice revealed the severely augmented expression level of COX-2 and iNOS colon tissue (Group II). The synthesized TK-CuNPs administered mice displayed the mild COX-2 and iNOS expression (Group III). Standard drug sulfasalazine treated mice also displayed a slight expression of COX-2 and iNOS (Group IV).

et al., 2015). MPO is a distinctive indicator of tissue injuries, neutrophil penetration, and inflammatory conditions. The status of MPO in the colon tissues depending upon the generation of superoxide anions implicates tissue necrosis and mucosal dysfunction (Han et al., 2015). Many preceding studies have highlighted that the DSS-challenge results in the augmented status of oxidative stress and MPO and also diminishes the cellular antioxidants status in the colon tissues (Yang et al., 2017). Previously, the augmented status of MPO was well reported in the DSS-triggered mice as a sign of neutrophils penetration, tissue injury, and mucosal disruption (Li et al., 2016). In this exploration, we noticed that the enzymatic action of MPO was augmented in the DSS-provoked mice than the control. However, the activity of MPO was appreciably suppressed by the administration of 10 mg/kg of TK-CuNPs.

The pro-inflammatory arbitrators like IL-1 β , IL-6, and TNF- α and its actions in the progression of IBD was extensively investigated, and these reports state that the extreme generation of pro-

inflammatory mediators can injure the colon mucosal layer and distress the intestinal homeostasis (Chi et al., 2018). It was also stated that the DSS-stimulated investigational colitis could be ameliorated through the neutralization of IL-1 β , IL-6, and TNF- α (Xiao et al., 2016). In this investigation, the augmented amount IL-1 β , IL-6, and TNF- α , was noted in the serum of DSS-triggered mice than control. Interestingly, the TK-CuNPs supplemented colitis mice exhibited appreciable diminution in the status of pro-inflammatory regulators.

Pro-inflammatory enzymes like iNOS and COX-2 were over-expressed at the inflammatory sites as a result the excessive TNF- α IL-6, and IL-1 β (Dai et al., 2018). It was reported that the COX-2 and iNOS are the imperative regulators of pro-inflammatory reactions activating the NF- κ B cascade in the inflamed colon tissues (Shen et al., 2015). The augmentation of COX-2 and iNOS are implicated, in response to the inflammatory conditions, to distress the integrity of colon mucosa (Zhou et al.,

2015). The tissue injuries can be ameliorated through the inhibition of COX-2 and iNOS, which are primarily generated via the inflammatory cells. The augmented status of pro-inflammatory mediators-regulated inflammatory cascades straightly influences the intestinal epithelial linings and results in the progression of IBD (He et al., 2016). The up-regulated COX-2 and iNOS expression were seen in a colon tissues of DSS-incited animals. Interestingly, COX-2 and iNOS expressions were suppressed by the TK-CuNPs administration.

The inflammatory cell penetrations like neutrophils in the colon during the progression of UC may accrete the vast amount of pro-inflammatory regulators like TNF- α , IL-1 β , and IL-6 (Jin et al., 2016). In this explorations, the histological analysis of colon tissues of DSS-induced mice has depicted increased damage in the epithelial linings and mucosa, severe inflammation, fibrosis, and leucocytes penetration. Interestingly, the TK-CuNPs administered colitis mice exhibited typical tissue architectures, epithelial linings, and cellular arrangements in the colon tissues. TK-CuNPs also prevented the penetration of leucocytes in the colon tissues. These findings coincided with the preceding report done by Balaha et al. (2016).

5. Conclusion

In conclusion, our findings from this exploration suggested that the formulated TK-CuNPs has the potential to alleviate the DSS-provoked acute colitis in mice through its anti-inflammatory properties. The supplementation of TK-CuNPs to the colitis induced mice showed the appreciable bodyweight gain, improved the colon length and spleen weight, suppressed the pro-inflammatory markers status, and down-regulated the COX-2 and iNOS expressions. These findings suggests that the TK-CuNPs could be a hopeful curative agent for colitis treatment. Nevertheless, additional investigations are still required to understand the precise mechanisms of TK-CuNPs against colitis.

Declaration of Competing Interest

The authors declare that they have no known competing financial interests or personal relationships that could have appeared to influence the work reported in this paper.

Acknowledgement

This project was supported by Researchers Supporting Project number (RSP-2021/230) King Saud University, Riyadh, Saudi Arabia.

Data Availability

The data used to support the findings of this study are available from the corresponding author upon request.

References

Balaha, M., Kandeel, S., Elwan, W., 2016. Garlic oil inhibits dextran sodium sulfate-induced ulcerative colitis in rats. *Life Sci J.* 146, 40–51.
 Balmus, I.M., Ciobica, A., Trifan, A., Stanciu, C., 2016. The implications of oxidative stress and antioxidant therapies in Inflammatory Bowel Disease: Clinical aspects and animal models. *Saudi J. Gastroenterol.* 22, 3–17.
 Beloqui, A., Coco, R., Pr at, V., 2016. Targeting inflammatory bowel diseases by nanocarriers loaded with small and biopharmaceutical anti-inflammatory drugs. *Curr. Pharm. Des.* 22, 6192–6206.
 Chae, H.-S., You, B.H., Song, J., Ko, H.W., Choi, Y.H., Chin, Y.-W., 2017. Mangosteen extract prevents dextran sulfate sodium-induced colitis in mice by suppressing NF- κ B activation and inflammation. *J. Med. Food* 20, 727–733.

Chi, J.-H., Seo, G.S., Lee, S.H., 2018. Oregonin inhibits inflammation and protects against barrier disruption in intestinal epithelial cells. *Int. Immunopharmacol.* 59, 134–140.
 Cooper, H.S., Murthy, S.N., Shah, R.S., Sedergran, D.J., 1993. Clinicopathologic study of dextran sulfate sodium experimental murine colitis. *Lab. Invest.* 69, 238–249.
 Cosnes, J., Gower-Rousseau, C., Seksik, P., Cortot, A., 2011. Epidemiology and natural history of inflammatory bowel diseases. *Gastroenterology* 140, 1785–1794.e4.
 Dai, Z., Feng, S., Liu, A., Wang, H., Zeng, X., Yang, C.S., 2018. Antiinflammatory effects of newly synthesized α -galacto-oligosaccharides on dextran sulfate sodium-induced colitis in C57BL/6J mice. *Food Res. Int.* 109, 350–357.
 Hagenlocher, Y., H sel, A., Bischoff, S.C., Lorentz, A., 2016. Cinnamon extract reduces symptoms, inflammatory mediators and mast cell markers in murine IL-10(-/-) colitis. *J. Nutr. Biochem.* 30, 85–92.
 Han, X., Jiang, X., Guo, L., Wang, Y., Veeraraghavan, V.P., Krishna Mohan, S., Wang, Z., Cao, D., 2019. Anticarcinogenic potential of gold nanoparticles synthesized from *Trichosanthes kirilowii* in colon cancer cells through the induction of apoptotic pathway. *Artif. Cells Nanomed. Biotechnol.* 47, 3577–3584.
 Han, F., Zhang, H., Xia, X.L., Xiong, H., Song, D., Zong, X., Wang, Y., 2015. Porcine β -defensin 2 attenuates inflammation and mucosal lesions in dextran sodium sulfate-induced colitis. *J. Immunol.* 194, 1882–1893.
 Harne, S., Sharma, A., Dhaygude, M., Joglekar, S., Kodam, K., Hudlikar, M., 2012. Novel route for rapid biosynthesis of copper nanoparticles using aqueous extract of *Calotropis procera* L. latex and their cytotoxicity on tumor cells. *Colloids Surf., B Biointerfaces* 95, 284–288.
 He, X., Wei, Z., Wang, J., Kou, J., Liu, W., Fu, Y., Yang, Z., 2016. Alpinetin attenuates inflammatory responses by suppressing TLR4 and NLRP3 signaling pathways in DSS-induced acute colitis. *Sci. Rep.* 6, 28370.
 Jin, Y., Lin, Y., Lin, L., Sun, Y., Zheng, C., 2016. Carcinoembryonic antigen related cellular adhesion molecule 1 alleviates dextran sulfate sodium-induced ulcerative colitis in mice. *Life Sci.* 149, 120–128.
 Katsanos, K.H., Papadakis, K.A., 2017. Inflammatory bowel disease: updates on molecular targets for biologics. *Gut Liver* 11, 455–463.
 Kim, S.R., Seo, H.S., Choi, H.S., Cho, S.G., Kim, Y.K., Hong, E.H., Shin, Y.C., Ko, S.G., 2013. Trichosantonin of STAT3 activity in breast cancer cells. *Evid. Complement. Altern. Med.*, 975350
 Lautreite, S., Bigot-Lasserre, D., Bars, R., et al., 2003. Optimization of cell based assays for medium through screening of oxidative stress. *Toxicol In Vitro* 17, 207–220.
 Lazarevic-Pasti, T., Leskovic, A., Vasic, V., 2015. Myeloperoxidase inhibitors as potential drugs. *Curr. Drug Metab.* 16, 168–190.
 Li, R., Chen, Y., Shi, M., Xu, X., Zhao, Y., Wu, X., et al., 2016. Gegen Qinlian decoction alleviates experimental colitis via suppressing TLR4/NF- κ B signaling and enhancing antioxidant effect. *Phytomedicine* 23, 1012–1020.
 Li, J., Chen, H., Wang, B., Cai, C., Yang, X., Chai, Z., Feng, W., 2017. ZnO nanoparticles act as supportive therapy in DSS-induced ulcerative colitis in mice by maintaining gut homeostasis and activating Nrf2 signaling. *Sci. Rep.* 7, 43126.
 Liu, F., Wang, B., Wang, Z., Yu, S., 2012. Trichosanthenin down-regulates Notch signaling and inhibits proliferation of the nasopharyngeal carcinoma cell line CNE2 in vitro. *Fitoterapia* 83, 838–842.
 Maqbool, Q., Iftikhar, S., Nazar, M., Abbas, F., Saleem, A., Hussain, T., Kausar, R., Anwaar, S., Jabeen, N., 2017. Green fabricated CuO nanobullets via *Olea europaea* leaf extract shows auspicious antimicrobial potential. *IET Nanobiotechnol.* 11, 463–468.
 Michielan, A., D'Inc , R., 2015. Intestinal permeability in inflammatory bowel disease: pathogenesis, clinical evaluation, and therapy of leaky gut. *Mediat. Inflamm.* 2015, 1–10.
 Mizoguchi, E., Low, D., Ezaki, Y., Okada, T., 2020. Recent updates on the basic mechanisms and pathogenesis of inflammatory bowel diseases in experimental animal models. *Intest. Res.* 18, 151–167.
 Mohammed, W.M., Mubark, T.H., Al-Haddad, R.M.S., 2018. Effect of CuO nanoparticles on antimicrobial activity prepared by sol-gel method. *Int. J. Appl. Eng. Res. Dev.* 13, 10559–10562.
 Mullane, K.M., Kraemer, R., Smith, B., 1985. Myeloperoxidase activity as a quantitative assessment of neutrophil infiltration into ischemic myocardium. *J. Pharmacol. Methods* 14, 157–167.
 Naraginti, S., Kumari, P.L., Das, R.K., Sivakumar, A., Patil, S.H., Andhalkar, V.V., 2016. Amelioration of excision wounds by topical application of green synthesized, formulated silver and gold nanoparticles in albino Wistar rats. *Mater. Sci. Eng., C* 62, 293–300.
 Riasat, R., Guangjun, N., Riasat, Z., Aslam, I., 2016. Effects of nanoparticles on gastrointestinal disorders and therapy. *J. Clin. Toxicol.* 6, 313.
 Seo, C.-S., Kim, T.-W., Kim, Y.-J., Park, S.-R., Ha, H., Shin, H.-K., Jung, J.-Y., 2015. *Trichosanthes kirilowii* ameliorates cisplatin-induced nephrotoxicity in both in vitro and in vivo. *Nat. Prod. Res.* 29, 554–557.
 Shen, Y., Sun, Z., Guo, X., 2015. Citral inhibits lipopolysaccharide-induced acute lung injury by activating PPAR- γ . *Eur. J. Pharmacol.* 747, 45–51.
 Tian, T., Wang, Z., Zhang, J., 2017. Pathomechanisms of oxidative stress in inflammatory bowel disease and potential antioxidant therapies. *Oxid. Med. Cell Long.* 2017, 1–18.
 Uranga, J.A., L pez-Miranda, V., Lomb , F., Abalo, R., 2016. Food, nutrients and nutraceuticals affecting the course of inflammatory bowel disease. *Pharmacol. Rep.* 68, 816–826.
 Xiao, Y.-T., Yan, W.-H., Cao, Y., Yan, J.-K., Cai, W., 2016. Neutralization of IL-6 and TNF- α ameliorates intestinal permeability in DSS-induced colitis. *Cytokine* 83, 189–192.

- Yang, N., Xia, Z., Shao, N., Li, B., Xue, L., Peng, Y., Zhi, F., Yang, Y., 2017. Carnosic acid prevents dextran sulfate sodium-induced acute colitis associated with the regulation of the Keap1/Nrf2 pathway. *Sci. Rep.* 7, 11036.
- Zhou, L.T., Wang, K.J., Li, L., Li, H., Geng, M., 2015. Pinoцемbrin inhibits lipopolysaccharide-induced inflammatory mediators production in BV2 microglial cells through suppression of PI3K/Akt/NF-kappaB pathway. *Eur. J. Pharmacol.* 761, 211–216.
- Zhu, H., Li, Y.R., 2012. Oxidative stress and redox signaling mechanisms of inflammatory bowel disease: updated experimental and clinical evidence. *Exp. Biol. Med.* 237, 474–480.